JOINT INSTITUTE FOR NUCLEAR RESEARCH
Bogoliubov Laboratory of Theoretical Physics (BLTP)

FINAL REPORT ON THE START PROGRAMME

Decay of the vortex muon

Supervisor:
Dr. Kotikov A. V.
BLTP, JINR, Dubna, Russia

Student:
Lavrenenko Valery, Belarus
Belarussian State University

Participation period:
July 07 – August 16

Dubna, 2025

Contents

Abstract

During the practice some properties of vortex states in high energy physics have been studied. The width of muon weak decay has been calculated in Born approximation for both polarized and unpolarized cases. The decay width of vortex state of unpolarized muon have been calculated for several sets of Bessel beam parameters. The analysis of the final electron energy distribution function and electron angular distribution function has been carried out.

Introduction

In particle physics, there are two elementary types of processes: the decay of a single particle and the scattering of two particles into an n-particle final state. Most complex real-world particle interactions in colliders can be described as sequential combinations of these elementary processes [1]. For most fields in the Standard Model, linearized equations describing "free" particles can be constructed. The solutions to these linearized equations are plane waves of varying algebraic structure, depending on the field type — scalar, spinor, vector, etc. — i.e., states with definite momentum and energy.

From an experimental perspective, quasi-monochromatic beams of elementary particles are the simplest to produce and control. Therefore, calculating decay widths and scattering cross-sections for particles with defined momenta remains a relevant and important task.

There exist more complex types of beams—twisted or vortex beams. In such beams, the projection of the momentum onto the beam's propagation direction is well-defined and is typically the dominant component; they are quasi-monochromatic. A distinctive feature of these beams is the presence of a non-zero component of the system's orbital angular momentum projection onto the propagation direction. This leads to an azimuthal phase dependence in the plane transverse to the beam's propagation direction. Examples of such beams include Bessel and Laguerre-Gauss beams.

Furthermore, since the field equations describing the propagation of such "free" particle beams are linear, these beams can be constructed as a linear combination of plane waves. Consequently, the decay width of a particle and the scattering cross-section become related to plane-wave case through an integral operator over the phase space of the initial beam.

This work is devoted to the calculation of the muon decay width in a Bessel beam. This process is well-known in the plane-wave case [2,3]. It has been study in application to vortex states under various approximations [4,5]. A similar process of neutron beta decay in the vortex state has also been actively studied in [6].

Amplitude and weak decay width of muon

According to modern concepts, the amplitude of the weak muon decay in the Born approximation has the form:

$$M_{if} = \bar{\mu}(\boldsymbol{p})(g_A + g_V\gamma^{\mu})\nu(q_1)\,\bar{e}(\boldsymbol{k})(g_A + g_V\gamma^{\nu})\tilde{\nu}(\boldsymbol{q_2})\frac{i\left(g_{\mu\nu}-\frac{q^{\mu}q^{\nu}}{M_W^2}\right)}{(p-q_1)^2-M_W^2+iM_W\Gamma_W}. \quad (1)$$

At energies much lower than the mass of the W bosons, the propagator of the vector boson field simplifies, and the amplitude reduces to the effective theory of four-fermion interaction proposed by Fermi:

$$M_{if} = 2\sqrt{2}G_F\bar{\mu}(\boldsymbol{p})\gamma^{\mu}\frac{(1-\gamma^5)}{2}\nu(\boldsymbol{q_1})\,\bar{e}(\boldsymbol{k})\gamma_{\mu}\frac{(1-\gamma^5)}{2}\tilde{\nu}(\boldsymbol{q_2}). \quad (2)$$

Let's assume that the muon in the initial state is polarized. This polarization can be described by specifying the corresponding bispinor. The expectation value of the spin operator is given by the spin 4-vector in this state:

$$s^{\mu} = \bar{u}(\boldsymbol{p})\frac{1}{2}\Sigma^{\mu}u(\boldsymbol{p}) = \left(\frac{(\boldsymbol{s}_{(0)}\boldsymbol{p})}{m}, \boldsymbol{s}_{(0)} + \frac{\boldsymbol{p}\,(\boldsymbol{s}_{(0)}\boldsymbol{p})}{m(p^0+m)}\right), \quad (3)$$

where $\boldsymbol{s}_{(0)}$ – is a three-component constant that coincides with the spatial part of the particle's spin vector in its rest frame.

The corresponding density matrix of the initial particle is given by:

$$u_s(\boldsymbol{p})\bar{u}_s(\boldsymbol{p}) = \frac{1}{2}(p^{\mu}\gamma_{\mu} + m)(1 + s^{\nu}\gamma^5\gamma_{\nu}). \quad (4)$$

Let's assume that we are not interested in the polarization state of the final particles. Then the density matrix of the final fermions takes the form:

$$\sum_{s=1,2} u_s(\boldsymbol{q_1})\bar{u}_s(\boldsymbol{q_1}) = (q_1^{\mu}\gamma_{\mu} + m_1) \quad (5a)$$

$$\sum_{s=1,2} u_s(\boldsymbol{k})\bar{u}_s(\boldsymbol{k}) = (k^{\mu}\gamma_{\mu} + m_e) \quad (5b)$$

$$\sum_{s=1,2} \mathrm{v}_s(\boldsymbol{q_2})\bar{\mathrm{v}}_s(\boldsymbol{q_2}) = (q_2^{\mu}\gamma_{\mu} - m_2) \quad (5c)$$

The decay width of the particle is constructed as follows [7]:

$$d\Gamma = \frac{1}{(2\pi)^5 2p^0}\left|M_{if}\right|^2\delta^4(p-k-q_1-q_2)\frac{d^3k}{2k^0}\frac{d^3q_1}{2q_1^0}\frac{d^3q_2}{2q_2^0} \quad (6)$$

Bessel beam case

The Bessel beam represents a state of a particle with a given energy, a projection of momentum in the propagating direction, a projection of orbital angular momentum in the same one, and a specified spin state. In a cylindrical coordinate system, where the z-axis is aligned with the beam direction, the expression for the fermion field takes the following forms in coordinate and momentum representations, respectively:

$$\psi_{\chi mk_z}(\boldsymbol{r}) = N_{Bes}J_m(\chi\, r_{\perp})e^{i(m\varphi+k_z z)}, \quad (7a)$$

$$\psi_{\chi mk_z}(\boldsymbol{k}) = \frac{N_{Bes}}{\sqrt{2E}}i^{-m}e^{im\varphi}\sqrt{\frac{2\pi}{\chi}}\delta^2(|k_{\perp}|-\chi)\delta(k-k_z). \quad (7b)$$

Parameter k_z defines the projection of momentum along the beam direction, χ— the projection of momentum perpendicular to the beam direction, $\hbar m$ — the projection of the particle's orbital angular momentum onto the beam direction, and the bispinor specifies the spin vector of the particle. Fig. 1 shows the distribution of

the squared modulus and phase of the particle's wave function in this state. The momentum representation of this state is an expansion in terms of plane waves.

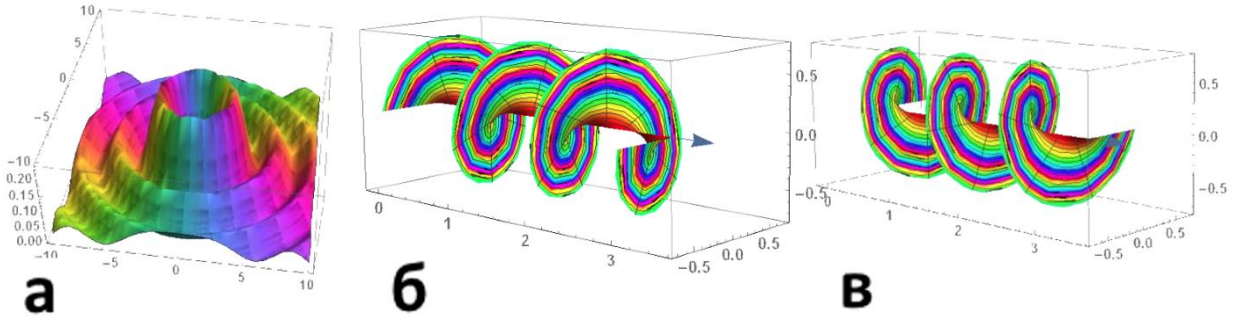

Figure 1. Bessel beam for a scalar particle. (a) Distribution of the squared modulus of the field $\psi_{\chi m k_z}$ n the plane perpendicular to the beam axis z for m = 2 and the phase indicated by color. It is clearly visible that the phase goes from 0 to 2π twice in one rotation around the axis. Constant phase surfaces of the twisted beam for (б) m = +1 and (в) m = −1. The color indicates the variation of the squared modulus of the field $\psi_{\chi m k_z}$.

The amplitude for a decaying particle in a superposition state is equal to the amplitude in the plane-wave case, integrated over the phase space of the initial state. To calculate decay cross-sections and widths, it is necessary to compute the square of the amplitude, which consists of a sum of amplitudes from different plane waves. Therefore, the final expression takes the form of a sum of squared amplitudes for different initial plane-wave states and interference terms between different initial plane-wave states. In the case of decay, the conservation of 4-momentum leads to the appearance of a product of two delta functions depending on the difference between the initial and the sum of final particle momenta. They are from the amplitude and its complex conjugate one. For the interference term between different plane waves, the sum of the final momenta is the same, as this quantity is determined by the selected point in phase space, while the initial momenta are different. Obviously, the product of these delta functions is always zero. Thus, for decay, as well as for scattering of two particles where only one particle is in a superposition state, the decay width or the corresponding cross-section is an averaging of the plane-wave decay width over the phase space of the initial particle. For Bessel beam case it leads to equation:

$$d\Gamma_{vortex} = \int d\Gamma_{PW} \frac{d\varphi}{2\pi} \qquad (8)$$

Squared matrix element evaluation

In this section, the exact expression for the squared amplitude of muon decay will be derived within the limit of the four-fermion interaction. The squared modulus of (2) takes the form:

$$\left|M_{if}\right|^2 = Sp\left(\rho(q_2)\left(\frac{1+\gamma^5}{2}\right)\gamma_\nu\rho(k)\gamma_\mu\left(\frac{1-\gamma^5}{2}\right)\right) \times Sp\left(\rho(q_1)\left(\frac{1+\gamma^5}{2}\right)\gamma^\nu\rho(p)\gamma^\mu\left(\frac{1-\gamma^5}{2}\right)\right). \quad (9)$$

Since the density matrices of the initial and final particles differ in form, it is convenient to perform the calculations for both factors separately. For the first factor, taking into account the form of the density matrices (5), one can obtain:

$$\begin{aligned} &Sp\left((q_2^\sigma\gamma_\sigma - m_2)\left(\frac{1+\gamma^5}{2}\right)\gamma_\nu\left(k^\rho\gamma_\rho + m_e\right)\gamma_\mu\left(\frac{1-\gamma^5}{2}\right)\right) \\ &= Sp\left((q_2^\sigma\gamma_\sigma)\left(\frac{1+\gamma^5}{2}\right)\gamma_\nu\left(k^\rho\gamma_\rho + m_e\right)\gamma_\mu\left(\frac{1-\gamma^5}{2}\right)\right) \\ &= Sp\left((q_2^\sigma\gamma_\sigma)\gamma_\nu\left(\frac{1-\gamma^5}{2}\right)\left(k^\rho\gamma_\rho + m_e\right)\left(\frac{1+\gamma^5}{2}\right)\gamma_\mu\right) \\ &= Sp\left(\left(\frac{1-\gamma^5}{2}\right)(q_2^\sigma\gamma_\sigma)\gamma_\nu\left(k^\rho\gamma_\rho\right)\gamma_\mu\right). \end{aligned} \quad (10)$$

Thus, for the unpolarized case, the mass of neutrinos and the electron does not explicitly enter the squared matrix element, yet it still manifests itself in the structure of the phase space of the final particles. The second factor, which includes the spin factor of the initial particle, takes a different form:

$$\begin{aligned} &Sp\left((q_1^\sigma\gamma_\sigma + m_1)\left(\frac{1+\gamma^5}{2}\right)\gamma^\nu\frac{1}{2}(p^\rho\gamma_\rho + m)(1+s^\tau\gamma^5\gamma_\tau)\gamma^\mu\left(\frac{1-\gamma^5}{2}\right)\right) \\ &= \frac{1}{2}Sp\left((q_1^\sigma\gamma_\sigma)\gamma^\nu\left(\frac{1-\gamma^5}{2}\right)(p^\rho\gamma_\rho + m)(1+s^\tau\gamma^5\gamma_\tau)\left(\frac{1+\gamma^5}{2}\right)\gamma^\mu\right) \\ &= \frac{1}{2}Sp\left(\left(\frac{1-\gamma^5}{2}\right)(q_1^\sigma\gamma_\sigma)\gamma^\nu(p^\rho - ms^\rho)\gamma_\rho\gamma^\mu\right). \end{aligned} \quad (11)$$

The expression, taking into account the mass of the particles, assumes the same form as the massless case if we make the substitution: $p^\mu \to p^\mu - ms^\mu$. Taking into account the relations $p^2 = m^2, s^2 = -1$ and $p^\mu s_\mu = 0$, one could obtain that vector $p^\mu - ms^\mu$ is isotropic.

Then, the squared amplitude of the process in the Born approximation, taking into account the masses of all four particles, has the form:

$$\left|M_{if}\right|^2 = 64G_F^2(kq_2)\big((p-ms)q_1\big). \quad (12)$$

Introduction of observables

Let us assume that detector can register only electrons, and can determine its momentum. In this case, the primary observable is the differential decay width with respect to the electron emission angle and energy:

$$\frac{d\Gamma}{d\Omega dk^0} = \frac{|\boldsymbol{k}|}{(2\pi)^5 4p^0}\int\left|M_{if}\right|^2\delta^4(p-k-q_1-q_2)\frac{d^3q_1}{2q_1^0}\frac{d^3q_2}{2q_2^0} \quad (13)$$

This quantity depends on the angle between the direction of the decaying particle's propagation and the direction of the emitted electron, the energy of the electron, the angle between the direction of the emitted electron and the spin of the decaying particle, as well as the initial parameters of the system. The energy of the electron in a certain direction takes on a continuous set of values, but is limited by a maximum energy that depends on the direction of the emitted electron.

Let us consider the detailed calculation of the integral in (13). Taking into account the form of the squared matrix element, one can express this integral as follows:

$$k^\mu(p-ms)^\nu\int q_{1\mu}q_{2\nu}\delta^4(q-q_1-q_2)\frac{d^3q_1}{2q_1^0}\frac{d^3q_2}{2q_2^0} = k^\mu(p-ms)^\nu f_{\mu\nu}(q^2;m_1,m_2). \quad (14)$$

The quantity $f_{\mu\nu}(q^2;m_1,m_2)$ can be expressed as a decomposition over all tensor structures of the same rank, constructed from primitives based on symmetry considerations. In this case, the only vector upon which this quantity depends is the vector q^μ. Thus, the general form of $f_{\mu\nu}(q^2;m_1,m_2)$ is:

$$f_{\mu\nu}(q^2;m_1,m_2) = \alpha(q^2)g_{\mu\nu} + \beta(q^2)\frac{q_\mu q_\nu}{q^2}. \quad (15)$$

Then, $\alpha(q^2)$ and $\beta(q^2)$ are the solution of the following system:

$$\begin{cases} f_\mu^\mu = 4\alpha+\beta = \frac{q^2-m_1^2-m_2^2}{2}R_2(q^2,m_1^2,m_2^2), \\ f_{\mu\nu}\frac{q^\mu q^\nu}{q^2} = \alpha+\beta = \frac{(q^2+m_1^2-m_2^2)(q^2-m_1^2+m_2^2)}{4q^2}R_2(q^2,m_1^2,m_2^2). \end{cases} \quad (16)$$

The final expression for $f_{\mu\nu}(q^2;m_1,m_2)$ is the following:

$$f_{\mu\nu}(q^2;m_1,m_2) = \frac{\pi}{24}\left(\left(q^2g_{\mu\nu}+2q_\mu q_\nu\right)+2\left(\Sigma\left(2\frac{q_\mu q_\nu}{q^2}-g_{\mu\nu}\right)-\frac{\Delta^2}{2q^2}\left(4\frac{q_\mu q_\nu}{q^2}-g_{\mu\nu}\right)\right)\right) \times\left(1-\frac{(m_1+m_2)^2}{q^2}\right)^{1/2}\left(1-\frac{(m_1-m_2)^2}{q^2}\right)^{1/2}, \quad (17)$$

where the following notation is used $\Sigma = m_1^2 + m_2^2$ and $\Delta = m_1^2 - m_2^2$. In the subsequent numerical analysis, we will assume the neutrinos to be massless. Then the previous expression will simplify significantly:

$$f_{\mu\nu}(q^2) = \frac{\pi}{24}\left(q^2 g_{\mu\nu} + 2q_\mu q_\nu\right). \quad (17')$$

The expression for the muon decay width, taking into account the mass of the electron, then has the form:

$$\frac{d\Gamma}{d\Omega dk^0} = \frac{G_F^2\,|\boldsymbol{k}|}{48\pi^4 p^0}\left[\Big((pk)\big(3m^2 - 4(pk)\big) - m(sk)\big(m^2 - 4(pk)\big)\Big) + m_e^2\big((3(pk) - 2m^2) - 3m(sk)\big)\right]. \quad (18)$$

The maximum energy of the electron, emitted in a certain direction, depends on the angle between the momentum of the initial particle and the momentum of the electron. The expression for the maximum energy of the electron, neglecting the masses of the neutrinos, is given by ($E_0 = p^0$):

$$E_e^{max} = \frac{m^2+m_e^2}{2E_0(1-\beta^2\cos^2(\theta)\,)}\left(1 + \sqrt{1 - (1-\beta^2\cos^2(\theta))\left(1 + \left(\frac{2E_0 m_e \beta\cos(\theta)}{m^2+m_e^2}\right)^2\right)}\right). \quad (19)$$

In the massless electron limit, which makes sense since the mass of the electron is 207 times smaller than the mass of the muon, the given formula simplifies significantly:

$$E_e^{max}(\theta) = \frac{m^2}{2E_0(1-\beta\cos(\theta))}. \quad (20)$$

From the form of the given expression, it is obvious that electrons with the maximum possible energy will be emitted in the direction of motion of the decaying particle; as the angle between the direction of the electron and the decaying particle increases, the maximum possible energy of the electron in the chosen direction will decrease.

When considering the decay of particles in a Bessel beam according to (8), the result will not differ in any way from the decay width of a set of incoherent particles flying apart from a certain point on the surface of a cone with the same apex angle θ_0. In this case, for particles flying in different directions, there will be their own maximum energy. Thus, two critical maximum energies appear $E_1 \leq E_2$:

$$E_1 = \frac{m^2}{2E_0(1-\beta\cos(\theta+\theta_0))}, \quad E_2 = \frac{m^2}{2E_0(1-\beta\cos(\theta-\theta_0))}. \quad (21)$$

The first quantity defines the threshold energy below which the electron could have been produced as a result of the decay of any of the initial particles. The second quantity corresponds to those electrons that were emitted along the direction of any initial muon, and represents the maximum possible energy of the emitted electron in the system. From (21), it is evident that in the limit $\theta_0 \to 0$, the kinematics of the Bessel beam transitions to the kinematics of a regular plane-wave one.

Of particular interest are the partial decay widths obtained by integrating (18) over the angle or over the electron energy over their entire range of variation, and the value of the total decay width. The total decay width in the rest frame of the

decaying massive particle is convenient as a normalization factor and can be simply calculated in the massless electron limit by integrating over the electron energy within $\{0, E_e^{max}(\theta)\}$, and then over the emission angle θ within $\{0, \pi\}$:

$$\Gamma_0 = \frac{G_F^2 m^5}{192\pi^3}. \quad (21)$$

Taking into account (8), it is convenient to introduce the following function for a Bessel beam:

$$w(E_e, \theta) = \frac{E_0}{m\Gamma_0} \int \frac{d\Gamma_{vortex}}{d\Omega dk^0}. \quad (22)$$

This function will be used for numerical analysis. Averaging the square of the matrix element leads to the cancellation of the phase factor in the wave function amplitude $\psi \sim e^{im\varphi}$. Thus, due to the absence of interference terms, the decay width does not depend on the orbital angular momentum carried by the beam. At the same time, the kinematic features of the beam significantly distinguish the considered case from that of a plane wave.

Numerical analysis

A numerical analysis was performed in the Wolfram Mathematica package. Within the framework of the numerical analysis, the unpolarized case of plane wave and Bessel beams was considered. For the numerical analysis, an initial muon energy of 3.1 GeV was chosen as a standard in the g-2 experiments and for verification purposes [4]. The electron spectra for two values of the cone opening angle θ_0 in the massless electron limit are presented in Fig. 2. Integration over the filling area yields the total decay width. In the blue region, all particles in the beam contribute to the integral, while in the red one only part of contributes. The peak corresponds to the emission of the final electron along the one of the muon momentum.

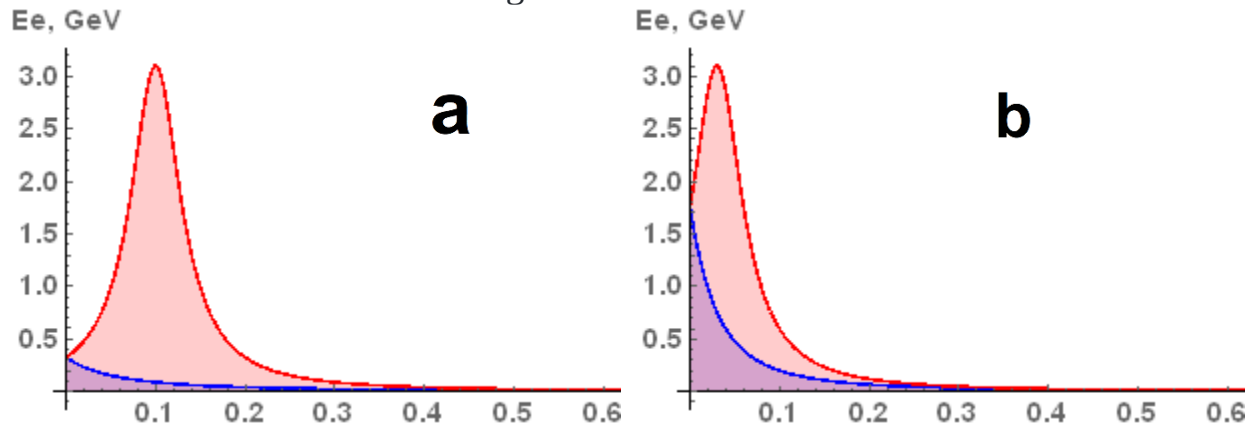

Figure 2. Electron spectra for two values of the cone opening angles a) $\theta_0 = 0.1$, b) $\theta_0 = 0.03$. The critical energy values of the electrons E_1 and E_2 are shown by solid lines.

It can be seen from the figure that the electron energy distributions at a fixed observation angle will always start from the minimum energy, which is zero in the massless electron limit. Behavior of the energy distribution function in the blue region will be determined by the contribution from all muons in the beam. Starting from energy E_1, only muons propagating in directions close to the electron emission direction make contribution to the energy distribution function value.

The angular distribution at a fixed value of the emitted electron energy also exhibits different behavior for high and low values of the final electron energy. An electron with energy $E_e < E_1(0)$ can be detected from zero angle relative to the beam propagation direction up to a certain critical angle. At energy $E_e > E_1(0)$, a final electron with a given energy can only be detected in the vicinity of the cone of the initial muon flight directions, and not along the beam propagation direction. The function $w(E_e, \theta)$, defined by relation (12), is presented in Fig. 3. The energy distributions of the final electrons and the angular distribution for two values of the opening angle and three values of the observation angles or final electron energies are presented in Fig. 4 and Fig. 5, respectively.

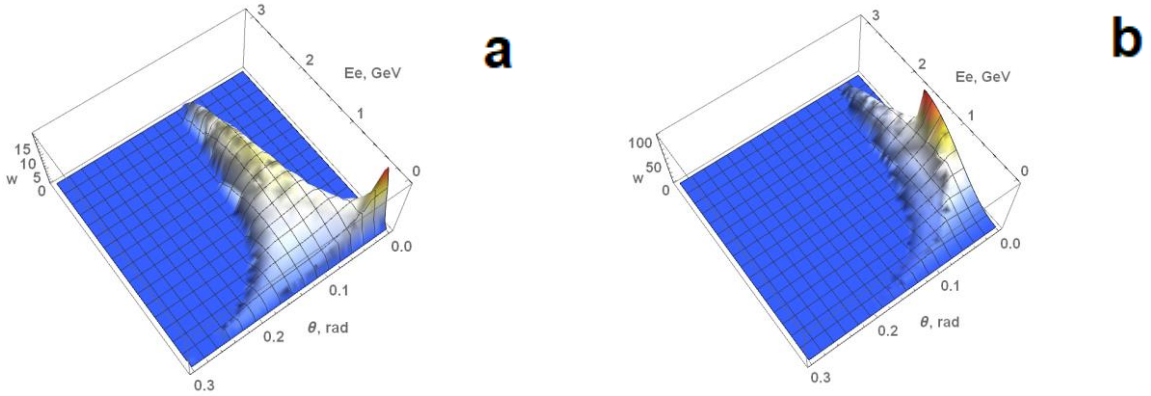

Figure 3. $w(E_e, \theta)$ as a function both parameters for two cases of cone opening angles: a) $\theta_0 = 0.1$, b) $\theta_0 = 0.03$.

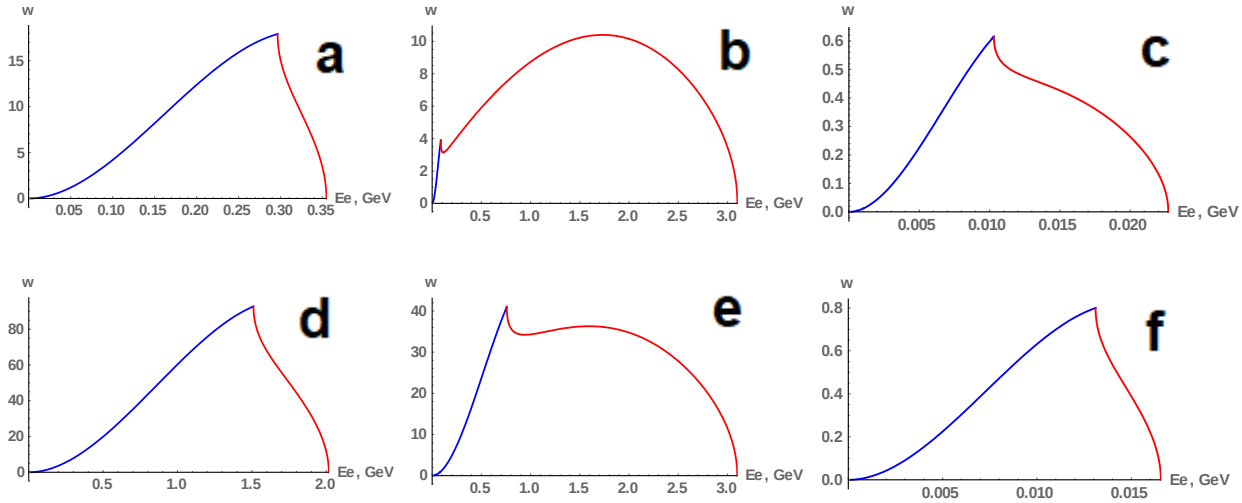

Figure 4. Electron energy distribution function (EEDF) for different cone opening angles and different directions of the emitted final electron. a) $\theta_0 = 0.1, \theta = 0.005$, b) $\theta_0 = 0.1, \theta = 0.1$, c) $\theta_0 = 0.1, \theta = 0.5$, d) $\theta_0 = 0.03, \theta = 0.005$, e) $\theta_0 = 0.03, \theta = 0.03$, f) $\theta_0 = 0.03, \theta = 0.5$.

From the provided distributions, it can be seen that at large deviations from the direction of the cone's axis, the behavior of the EEDF is similar both inside and outside the cone (Fig. 4 a, c and d, f). Near the cone's axis, the behavior of the EEDF is primarily determined by muons propagating in directions close to the observation direction.

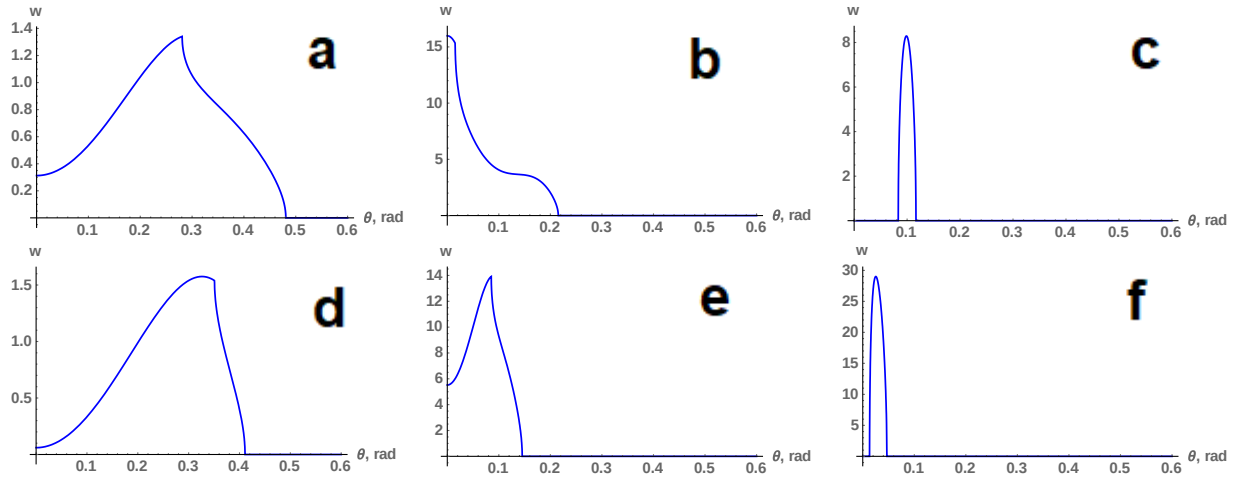

Figure 5. Angular electron distribution function for different cone opening angles and different directions of the emitted final electron. a) $\theta_0 = 0.1, E_e = 0.025$, b) $\theta_0 = 0.1, E_e = 0.25$, c) $\theta_0 = 0.1, E_e = 2.5$, d) $\theta_0 = 0.03, E_e = 0.025$, e) $\theta_0 = 0.03, E_e = 0.25$, f) $\theta_0 = 0.03, E_e = 2.5$.

The presence of a kink in the distribution functions serves as a highly indicative marker of a non-plane-wave beam. Of particular interest is the robustness of this marker against blurring of the cone opening angle. The results of the robustness evaluation are shown in Fig. 6. Integration over the angle θ_0 could only be performed numerically within finite limits.

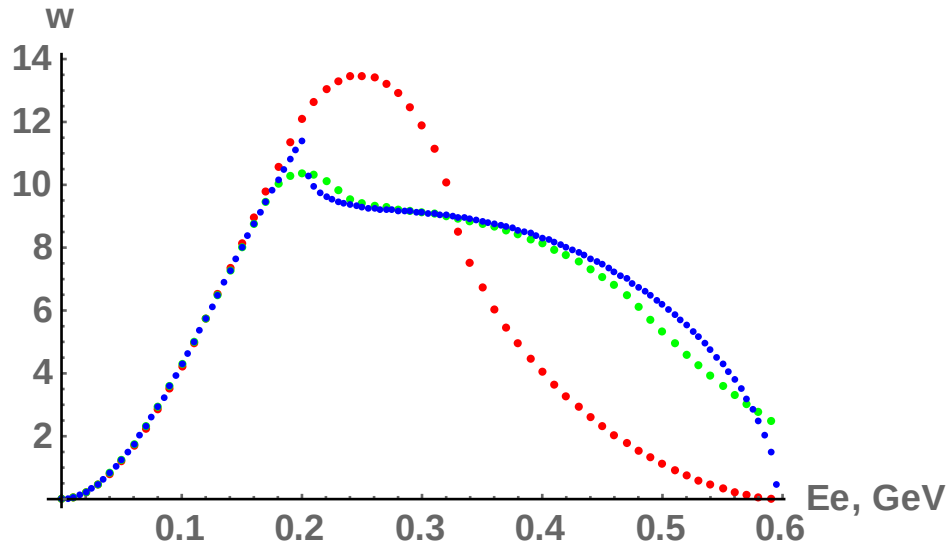

Figure 6. EEDF is shown by blue color for $\theta_0 = 0.03, \theta = 0.1$, by green one for averaging over θ_0 in the limits of {0.03-0.01, 0.03+0.01}, by red one for the case of «filled» cone, i. g. averaging over θ_0 in the limits of {0, 0.03}.

From the provided figure, it can be seen that averaging smooths out the kink; however, the shape of the distribution still retains a distinctive form.

Taking into account the mass of the electron in the decay at these energies does not significantly alter the overall picture. The results of this consideration are presented in Fig. 7. The large dips in the graph representing the difference between the two distribution functions correspond to the regions of the kink in the graph and the area of maximum energy. These dips can be explained, firstly, by the dependence

of the critical energies E_1, and E_2 on the mass of the electron, and secondly, by the nearly vertical nature of the function itself in the vicinity of these points, meaning that a small deviation along the horizontal axis causes a significant change in the function. For all intermediate energies, the relative effect is on the order of 0.1%.

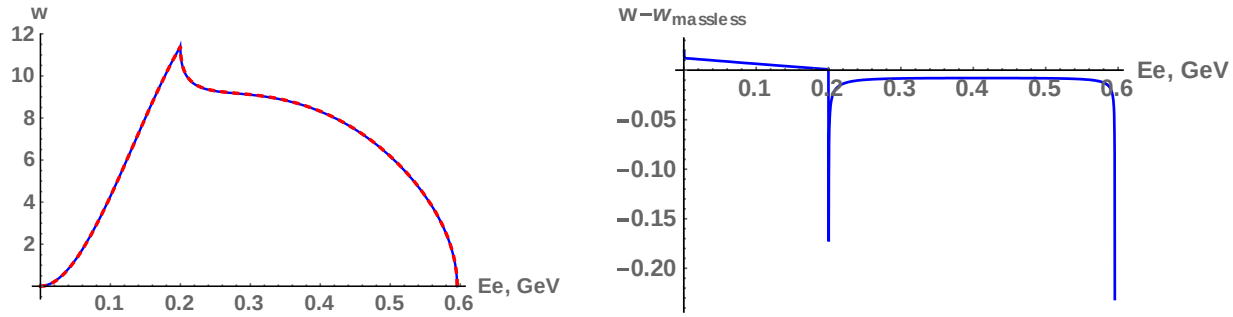

Figure 8. Correction to the EEDF with respect to electron mass for parameters $E_0 = 3.1\ GeV, \theta_0 = 0.03, \theta = 0.1$.

Conclusion

During the practice, the main focus was on exact calculation of the weak decay width of muon in Born approximation. This value has been calculated taking into account non-zero masses of all final particles. This results can be applied for neutron weak decay, too.

The influence of non-plane-wave state of the initial particle on decay width has been investigated. It was shown that there are no interference terms in decay width between different plane-waves the initial state is decomposed on. So, any superposition state of initial particle in decay-type process is similar to simple non-coherent union of particles with the similar momentum distribution. However, in contrast to this case, a vortex beam has one attractive property. It is topologically protected from the diffraction and is more stable than just union of uncoherent particles with the same momentum distribution. But all features of decay width behavior are governed just by kinematics of the current process.

It will be interesting to deal with the scattering process with two initial particles in superposition states. The interference terms of squared amplitude could make large effort on differential cross section in special cases.

References

1. Peskin M. E. An Introduction to Quantum Field Theory/ M. E. Peskin, D. V. Schroeder. – Addison-WesleyPublishing Company, 1995. – 784.
2. M. Giannini, Muon decay and neutrino mass. – 2022, arXiv:2207.02717v1.
3. M. Giannini, An improved upper limit for the (muon based) neutrino mass. – 2022, arXiv:02718v1.
4. P. Zhao, I. Ivanov, P. Zhang, Decay of the vortex muon. – 2024, arXiv:2106.00345v3.
5. P. Zhao, Z_n symmetry in the vortex muon decay. – 2022, arXiv:2204.13351v2.
6. W. Kou, B. Guo, X. Chen, Unveiling the Secrets of Vortex Neutron Decay. – 2024, arXiv:2407.06520v1.
7. Byckling, E. Particle Kinematics/ E. Byckling, K. Kajantie. – London: John Wiley and sons, 1973. – 343.

Acknowledgments

I would like to express my sincere gratitude to Dr. Kotikov for the excellent organization of practice including careful planning, attention to details and methodological guidance. His deep and individual approach to student guidance led to the successful completion of all tasks.

I would like to express my heartfelt appreciation to organizers of JINR START program. The enormous organizational work they have done has allowed me to focus my main efforts on scientific work in a favorable atmosphere.